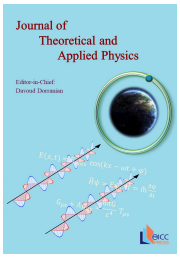

Volume 17, Issue 4, 172343 (1-7)

Journal of Theoretical and Applied Physics (JTAP)

https://dx.doi.org/10.57647/j.jtap.2023.1704.43

Role of dust on the gradient driven instability in an E × B plasma

Munish [1], Dimple Sharma [2]*, Babu Lal [3], Sukhmander Singh [4]

[1]*Department of Physics, Gargi College, University of Delhi, Delhi, India.*
[2]*Department of Physics, Atma Ram Sanatan Dharma College, University of Delhi, Delhi, India.*
[3]*Department of Physics, Swami Sharaddhanand College Alipur, University of Delhi, India.*
[4]*Department of Physics, Central University of Rajasthan, Ajmer, India.*

***Corresponding author**: sharma14dimple@gmail.com

Received 25 May 2023; Accepted 01 June 2023; Published online 05 June 2023

Abstract:
The **E** × **B** plasma systems play an important role in the technologies like electric space propulsion and magnetized plasma sources used in plasma material interaction/surface processing. However, due to the gradient in plasma density, collisions and external fields such systems become prone to the instabilities and also dust particles are generated during the plasma processing. Hence, this article discusses the growth of gradient driven instability in a cross-field plasma, where both the ions and the electrons are magnetized and dust particles also exist. Using the fluid approach, we write basic equations and then derive an equation in terms of perturbed potential. The unperturbed part of this equation leads to the dispersion equation which is solved numerically for obtaining the growth rate of the instability. The normalized form of the growth rate is investigated in greater detail under the effect of dust density, dust mass, dust temperature, external magnetic field, ion temperature and ion temperature gradient.

Keywords: **E** × **B** plasma systems; Temperature gradient; Dust particles; Dust mass; Gradient driven instability; Plasma processing; Space propulsion; Film deposition

1. Introduction

Dust is the mixture of complex ions and neutrals that are present in the plasma. Very early studies gave evidence that the dust particles are often found in the bottom areas of **E** × **B** systems such as Tokamaks, Stellarators and Hall thrusters [1]. Presence of dust and its levitation in the plasma affect the plasma properties by charging effects of dust grains etc. Hollenstein et al. have done a detailed study on the existence, growth and plasma confinement of nano- and microparticles in these systems [2]. Consequences of dust levitation and its charging effects in the plasma in the **E** × **B** systems are matter of discussion for long as they degrade the systems and are thereby affecting their performance [3]. Many studies have been carried out to observe the effect of dust in the plasma for various nonlinear phenomena. For example, Malik et al. showed that the soliton amplitude gets reduced with increase in dust mass and charge; however, presence of more electrons amplifies the soliton amplitude. Different kinds of instabilities also develop due to the presence of dust particles in the Hall thrusters [4]. In this direction, Malik et al. have investigated the Rayleigh instability in a Hall thruster channel in the presence of dust [5]. Many different types of instabilities have been found to exist because of dust in the plasma chambers of the system. Lazurenko et al. studied high frequency instabilities which exist towards the exit region of the thrusters [6]. Long-wavelength gradient drift instabilities has been studied by Smolyakov et al. [7] and Frias et al. [8]. A peculiar type of instability known as rotating spoke instability in annular Hall thrusters has been reported by Chesta et al. [9] and Parker et al. [10]. Litvak et al. [11] have recorded high-frequency instability experimentally in the range 5-10 MHz. Kapulkin and Guelman [12] presented a theoretical model for analysing low frequency instabilities and they observed non-uniformity in the plasma and magnetic field both these factors give rise to instabilities. Godall has made fast camera observations to see the impact of dust particles in the **E** × **B** system devices, such as Tokamaks, which is the thermal glow and line radiation of ablated and

excited atoms, such illumination inside the plasma can be seen during heavy plasma surface interaction [13]. Dust can attain charge on the surface of supersonically moving aircraft, leading to the formation of unstable plasma [14–16]. Hall thruster carries the cross-field plasma, where the axial electric field accelerates the heavy ions that provides the thrust to the space vehicle. However, due to the gradients in the density and magnetic field, and collisions between the electrons and neutral atoms in such systems may lead to different kinds of the instabilities [17–20]. The ordinary dusty plasma can also support Rayleigh instability driven by the gradient [21]. The instabilities generally disturb the mechanism of the thrust generation in Hall thrusters or other $\mathbf{E}\times\mathbf{B}$ systems. Hence, recently, there has been a focus on the profile of the magnetic field for achieving a controlled divergence of the plasma plume emerging from the space vehicle or the magnetic nozzle [22]. Not only this special profile of the magnetic field has been found to enhance the thrust and efficiency [23–25]. The magnetic field has been found to play a vital role in other fields of radiation as well [26].

The presence of dust in the Hall thruster channel has been found to influence the Rayleigh-Taylor instability [5, 27] and resistive instability [28]. The position of dust whether inside or outside the channel also plays a vital role in suppression of the instabilities [5]. However, these observations are limited to the Hall thruster plasmas where only the electrons are magnetized. It would be the point of interest to see whether the dust impact remains the same on the growth rate of the instability when the ions are also magnetized, means when we talk about $\mathbf{E}\times\mathbf{B}$ systems which are used in plasma processing. Hence, the objective of this article is to derive an equation in terms of the perturbed potential based on which we get a dispersion equation. The dispersion equation is solved to get the growth rate of the instability which is driven by the density gradient. This instability obtained in the present plasma model is similar to the Rayleigh instability.

2. Formulation of the problem

In the present study, the magnetic field is applied ($\mathbf{B}$) in the z-direction due to which both the species, i.e., ions and electrons are assumed to be magnetized. As both ions and electrons have finite temperature, therefore a non-zero pressure-gradient term will exist, which is taken in to account through their respective fluid equations. Consequently, the motion of both the ions and the electrons will be affected by the $\mathbf{E}\times\mathbf{B}$ drifts.

In the basic equations, n_j is the density, T_j is the temperature and m_j is the mass of the electrons ($j=e$) and ions ($j=i$). U and V, respectively, depict the velocities of the electrons and the ions. Ze and e are the charges of the ions and the electrons, respectively. The un-perturbed and oscillating part of densities are represented by (n_{i0}, n_{e0}) and (n_{i1}, n_{e1}), respectively. The x- and y-components of unperturbed and oscillating parts of velocities are expressed by $(V_{x0}, U_{x0}, V_{y0}, U_{y0})$ and $(V_{x1}, U_{x1}, V_{y1}, U_{y1})$, respectively. The electric field has its oscillating value equal to $\mathbf{E}_1$ and associated potential is φ_1. The fundamental equations for the given system are the continuity equations and equations of motion for both the electrons and the ions. Poisson's equation reveals the relationship of plasma species densities with the electric potential. In linearized form, the said equations read

A. For electrons

(i) Continuity equation

$$\partial_t n_{e1} + n_{e0}\partial_x U_{x1} + n_{e0}\partial_y U_{y1} + U_{x1}\partial_x n_{e0} + U_{y0}\partial_y n_{e1} = 0 \tag{1}$$

(ii) X-component of equation of motion

$$\partial_t U_{x1} + U_{y0},\partial_y U_{x1} = \frac{e}{m_e},\partial_x\varphi_1 - \frac{e}{m_e},(U_{y0}+U_{y1})(B_0) - \frac{2T_e}{m_e n_e},\partial_x n_{e0} - \frac{2T_e}{m_e n_e},\partial_x n_{e1} - \frac{2}{m_e}\partial_x T_e \tag{2}$$

(iii) Y-component of the equation of motion

$$\partial_t U_{y1} + U_{x1},\partial_x U_{y0} + U_{y0},\partial_y U_{y1} = \Omega_e U_{x1} - \frac{2T_e}{m_e n_e}, \partial_y n_{e1} + \frac{e}{m_e},\partial_y\varphi_1 \tag{3}$$

B. For ions:

(iv) Continuity equation

$$\partial_t n_{i1} + n_{i0}\partial_x V_{x1} + V_{x1}\partial_x n_{i0} + n_{i0}\partial_y V_{y1} + V_{y0}\partial_y n_{i1} = 0 \tag{4}$$

(v) X-component of the equation of motion

$$\partial_t V_{x1} + V_{y0}\partial_y V_{x1} = -\frac{Ze}{m_i}\partial_x\varphi_1 + \frac{Ze}{m_i},(V_{y0}+V_{y1})(B_0) - \frac{2T_i}{m_i n_i},(\partial_x n_{i0} + \partial_x n_{i1}) - \frac{2}{m_i}\partial_x T_i \tag{5}$$

(vi) Y-component of the equation of motion

$$\partial_t V_{y1} + V_{x1}\partial_x V_{y0} + V_{y0}\partial_y V_{y1} = -\frac{Ze}{m_i},\partial_y\varphi_1 - \frac{Ze}{m_i}, V_{x1}(B_0) - \frac{2T_i}{m_i n_i},\partial_y n_{i1} \tag{6}$$

C. For dust:

$$\partial_t n_{d1} + \mathrm{v}_{d0}\partial_x n_{d0} + \mathrm{v}_{d1x}\partial_x n_{d0} + \mathrm{v}_{d0}\partial_x n_{d1} + n_{d0}(\boldsymbol{\nabla},\mathbf{v}_{d1}) = 0 \tag{7}$$

$$\partial_t \mathrm{v}_{d1} + \mathrm{v}_{d0}\partial_x v_{d1} = \frac{eZ_d}{m_d}\mathbf{E}_1 - \frac{\boldsymbol{\nabla} p_d}{m_d n_{d0}} \tag{8}$$

In Eqs. (1)-(8), ∂_t, ∂_x and ∂_y are the first-order derivatives with respect to time, x and y, respectively. Moreover, a factor of 2 appears in the equation of motions because of number of degrees of freedom of the ions and electrons. This factor is actually the ratio of specific heats at constant pressure and constant volume C_P/C_V.

3. Derivation of dispersion equation

We take $\Omega_i = eB_0/m_i$ and $\Omega_e = eB_0/m_e$ as the ion-cyclotron and electron-cyclotron frequencies, respectively. Considering ∂_x^2 and ∂_t^2, respectively, as the second-order derivatives with respect to x-axis and time and taking $\acute{A} = i\omega - ikU_{y0}$

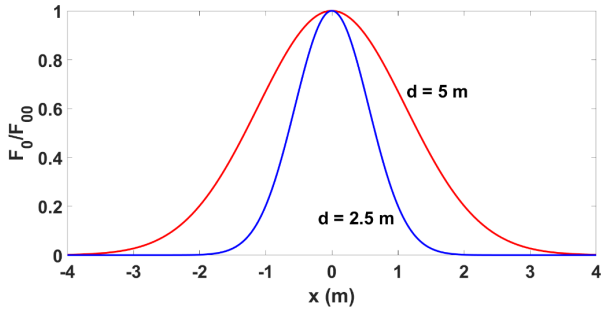

Figure 1. Variation of quality F_0/F_{00} with the distance x, showing the impact of parameter d.

and $\acute{B} = 1+(2T_e k^2)/(\acute{A} m_e \omega)$ with k is the wavenumber corresponding to the oscillations of the wavelength λ, and ω_e as the electron-plasma frequency, given by $(n_{e0}e^2/m_e\varepsilon_0)^{1/2}$, we derive expression in terms of these quantities. Further, we take $A_1 = i\omega - ikV_{y0}$ and $B_1 = 1+(2T_i k^2)/(A_1 m_i \omega)$. ω_i is the ion-plasma frequency, given by $(n_{i0}e^2/m_i\varepsilon_0)^{1/2}$. The oscillating densities of the electrons and the ions are obtained solving Eqs. (1)-(8) in terms of the perturbed potential. Then those expressions are put in the following Poison's equation which reveals the relationship between plasma species densities and the electric potential

$$\varepsilon_0(\partial_x^2+\partial_y^2)\varphi_1 = e(n_{e1}+Zn_{i1}+Z_d n_{d1}) \tag{9}$$

This equation with the substitution of the expressions of the perturbed densities of the electron fluid, ion fluid and dust fluid leads to the following equation:

$$\begin{aligned}
&(\partial_x^2\varphi_1 - k^2\phi_1) + \partial_x^2\varphi_1 \\
&\left[\frac{n_{e0}e^2}{X_1\acute{A}\acute{B}\varepsilon_0 m_e\omega_e} - \frac{Z^2e^2n_{i0}}{S_1A_1B_1m_i\omega_i\varepsilon_0} - \frac{Z_d^2e^2n_{d0}}{\varepsilon_0(M_d\omega^2-\gamma_d T_d k_y^2)}\right] \\
&+k^2\phi_1\left(\frac{Z^2e^2n_{i0}\omega_i}{A_1B_1m_i\Omega_i^2\varepsilon_0} + \frac{Z_d^2e^2n_{d0}}{\varepsilon_0(M_d\omega^2-\gamma_d T_d k_y^2)}\right) \\
&+\phi_1\left[\frac{ZeikP_1\omega_i}{Q_1m_i\Omega_i^2} - \frac{ikT_1\omega_e e}{U_1m_e\Omega_e^2} + \frac{V_1e^2B_0ik}{W_1X_1m_e^2\omega_e}\right] \\
&+\left[-\frac{\alpha n_{e0}e}{\acute{A}\acute{B}\varepsilon_0} + \frac{Ze\alpha n_{i0}}{A_1B_1\varepsilon_0} - \frac{2T_iP_1}{Q_1m_in_{i0}\Omega_i}\partial_x n_{i0}\right. \\
&-\frac{2P_1}{Q_1m_i\Omega_i}\partial_x T_i - \frac{2T_iP_1ZeB_0}{Q_1m_i^2\Omega_i^2n_{i0}}\partial_x n_{i0} - \frac{2P_1ZeB_0}{Q_1m_i^2\Omega_i^2}\partial_x T_i \\
&+\frac{2T_iZeik}{A_1B_1m_i\Omega_i\varepsilon_0}\partial_x n_{i0} + \frac{2ikn_{i0}Ze}{A_1B_1m_i\Omega_i\varepsilon_0}\partial_x T_i \\
&+\frac{2ikZ^2e^2T_iB_0}{A_1B_1m_i^2\Omega_i^2\varepsilon_0}\partial_x n_{i0} + \frac{2ikZ^2e^2n_{i0}B_0}{A_1B_1m_i^2\Omega_i^2\varepsilon_0}\partial_x T_i + \\
&+\frac{2ikn_{i0}Ze}{A_1B_1m_i\Omega_i^2\varepsilon_0}\partial_x T_i\partial_x V_{y0} + \frac{2R_1KT_i}{S_1^2en_{i0}}\partial_x n_{i0} \\
&+\frac{2V_1T_e}{W_1X_1m_en_{e0}\omega_e}\partial_x n_{e0} - \frac{2P_1T_iik\omega_i}{Q_1m_i\Omega_i^2} + \frac{2V_1T_eikB_0e}{W_1X_1m_e^2\omega_e^2} \\
&\left.+\frac{eZ_d^2\gamma_d T_d}{\varepsilon_0(M_d\omega^2-\gamma_d T_d k_y^2)}\partial_x^2 n_{d0}\right] = 0.
\end{aligned} \tag{10}$$

The coefficients and the constants used in Eq. (10) are stated as follows

$$\begin{aligned}
P_1 &= 3+\frac{Z^2e^2ikn_{i0}B_0}{A_1B_1m_i\Omega_i^2\varepsilon_0}\partial_x V_{y0} + \frac{2Z_dek_dn_{d0}}{\omega B_d\varepsilon_0}, \\
Q_1 &= 4+\frac{ZeB_0}{m_i\Omega_i^2}\partial_x V_{y0}, \\
R_1 &= \frac{\Omega_i}{\omega_i^2}\partial_x^2 V_{y0} + \frac{ZeB_0}{m_i\omega_i^2}\partial_x^2 V_{y0}, \\
S_1 &= 1+\frac{\Omega_i^2}{\omega_i^2} + \frac{2ZeB_0\Omega_i}{m_i\omega_i^2} + 2\frac{\Omega_i}{\omega_i^2}\partial_x V_{y0} + \frac{Z^2e^2B_0^2}{m_i^2\omega_i^2}, \\
T_1 &= \frac{ikn_{e0}e^2B_0}{\acute{A}\acute{B}m_e\Omega_e^2\varepsilon_0}\partial_x U_{y0} + \frac{3ikn_{e0}e}{\acute{A}\acute{B}\varepsilon_0} + \frac{kn_{d0}Z_de}{\omega B_d\varepsilon_0}, \\
U_1 &= 1-\frac{eB_0}{m_e\Omega_e^2}\partial_x U_{y0} + \frac{2eB_0}{m_e\Omega_e}, \\
V_1 &= \frac{n_{e0}e\Omega_e}{\acute{A}\acute{B}\varepsilon_0\omega_e^2}\partial_x^2 U_{y0} + \frac{n_{e0}B_0e^2}{\acute{A}\acute{B}\varepsilon_0m_e\omega_e^2}\partial_x^2 U_{y0}, \\
W_1 &= 1+\frac{4\Omega_e^2}{\omega_e^2} - \frac{2\Omega_e}{\omega_e^2}\partial_x U_{y0}, \\
X_1 &= 1+\frac{4\Omega_e^2}{\omega_e^2} - \frac{eB_0}{m_e\omega_e^2}\partial_x U_{y0}.
\end{aligned}$$

Inside the thruster's chamber, the ion and the electron densities, also the ion and the electron drift velocities are assumed to vary according to the expression $F_0 = F_{00}\exp[-10(x/d)^2]$. Here, the peak value of n_{e0}, n_{i0}, n_{d0}, U_{i0} and V_{i0} is represented by F_{00}. Such a distribution may occur when the ionization takes place in one end of the chamber of plasma devices. The variation of quantity F_0 is shown in Fig. 1, which resembles the Gaussian distribution of the said quantity. Clearly the width of the distribution enhances with the value of d, which is taken as 2.5 m and 5 m in the figure. The increasing width means the spatial variation of the said quantity is slow and hence, a wreaker gradient exists in that case.
Using the above velocities and densities profiles [5, 29, 30], the un-perturbed part of Eq. (10) has been solved to find the growth rate of the instability. This finally gives the following dispersion equation

$$g_1\omega^6 + g_2\omega^5 + g_3\omega^4 + g_4\omega^3 + g_5\omega^2 + g_6\omega + g_7 = 0. \tag{11}$$

Various coefficients used in the above equation are given below:

$$\begin{aligned}
g_1 &= QLiF \\
g_2 &= B_2iLF + QL\acute{X} + QKiF, \\
g_3 &= A_2LFi + B_2L\acute{X} + B_2KFi + QL\acute{Y} + QK\acute{X}, \\
g_4 &= A_2L\acute{X} + A_2KFi + B_2L\acute{Y} + QL\acute{Z} + Q\acute{Y}K + PIC_2Li, \\
g_5 &= A_2L\acute{Y} + A_2K\acute{X} + B_2L\acute{Z} + B_2K\acute{Y} + QK\acute{Z} + PIC_2Ki \\
&\quad - BNLPIi + PIDC_2L, \\
g_6 &= A_2L\acute{Z} + A_2K\acute{Y} + B_2K\acute{Z} - BNKPIi + PIDC_2K - PIDBNL, \\
g_7 &= A_2K\acute{Z} - PIDBNK.
\end{aligned}$$

In these coefficients, we have made use of the following quantities

$$
\begin{aligned}
A_2 &= MN - QN^2 \\
B_2 &= Mi - 2iNQ \\
C_2 &= AN - Bi \\
\acute{X} &= iG = CF + EF \\
\acute{Y} &= iH + CG + EG \\
\acute{Z} &= CH + EH \\
P &= \frac{2T_e k_e}{m_e \varepsilon_0}\partial_x n_{e0} + \frac{2T_d kd}{m_d \varepsilon_0}\partial_x n_{d0}, \\
N &= -ikV_{y0}
\end{aligned}
$$

If we assume

$$
\Lambda = \frac{2Z^2 e^2 ikn_{i0}B_0}{m_i \Omega_i \varepsilon_0} + \frac{Z^2 e^2 ikn_{i0}B_0}{m_i \Omega_i^2 \varepsilon_0}\partial_x V_{y0} + \frac{2Z_d e k_d n_{d0}}{\varepsilon_0},
$$

then the other coefficients are written as follows:

$$
\begin{aligned}
Q =& \frac{2T_i ik}{\acute{Q} m_i \Omega_i^2}\left[\frac{2Z^2 e^2 ikn_{i0}B_0}{m_i \Omega_i \varepsilon_0} + \frac{Z^2 e^2 ikn_{i0}B_0}{m_i \Omega_i^2 \varepsilon_0}\partial_x V_{y0}\right. \\
&\left. + \frac{2Z_d e k_d n_{d0}}{\varepsilon_0}\right] \\
M =& \frac{2T_i Zeik}{m_i \Omega_i \varepsilon_0}\partial_x n_{i0} + \frac{2ikZ^2 e^2 T_i B_0}{m_i^2 \Omega_i^2 \varepsilon_0}\partial_x n_{i0} + \frac{2ikn_{i0}Ze}{m_i \Omega_i \varepsilon_0}\partial_x T_i \\
&+ \frac{2Z^2 e^2 ikn_{i0}B_0}{m_i^2 \Omega_i^2 \varepsilon_0}\partial_x T_i + \frac{2ikn_{i0}Ze}{m_i \Omega_i^2 \varepsilon_0}\partial_x V_{y0}\partial_x T_i \\
&+ \left[\frac{2Z^2 e^2 ikn_{i0}B_0}{m_i \Omega_i \varepsilon_0} + \frac{Z^2 e^2 ikn_{i0}B_0}{m_i \Omega_i^2 \varepsilon_0}\partial_x V_{y0} + \frac{2Z_d e k_d n_{d0}}{\varepsilon_0}\right] \\
&\left[-\frac{2T_i}{\acute{Q} m_i n_{i0} \Omega_i}\partial_x n_{i0} - \frac{2T_i ZeB_0}{\acute{Q} m_i^2 \Omega_i^2 n_{i0}} - \frac{2}{\acute{Q} m_i}\partial_x T_i - \frac{2ZeB_0}{\acute{Q} m_i^2 \Omega_i^2}\partial_x T_i\right]
\end{aligned}
$$

$$
\begin{aligned}
\acute{Q} =& 1 + \frac{2ZeB_0}{m_i \Omega_i} + \frac{Z^2 e^2 B_0^2}{m_i^2 \Omega_i^2} + \frac{ZeB_0}{m_i \Omega_i^2}\partial_x V_{y0}, \\
L =& i + \frac{2T_e k^2}{m_e \Omega_e^2}, \quad K = -\frac{2T_e k^2 ikU_{y0}}{m_e \Omega_e^2} - ikU_{y0}, \\
J =& 2eB_0 \Omega_e m_e + 2e^2 B_0^2 - 2eB_0 m_e \partial_x U_{y0}, \\
I =& m_e n_{e0} \Omega_e^2, \quad H = -ikU_{y0} m_e n_{e0} \Omega_e^2 D - 2T_e k^2 n_{e0}(k^2 U_{y0}^2), \\
G =& iDm_e n_{e0} \Omega_e^2 - 4T_e k^3 n_{e0} U_{y0} + kU_{y0} m_e n_{e0} \Omega_e^2, \\
F =& -2T_e k^2 n_{e0} - 2T_d k_d^2 n_{d0} - m_e n_{e0} \Omega_e^2, \\
E =& \frac{e^2 B_0^2 - eB_0 m_e \partial_x U_{y0}}{m_e^2 \Omega_e}, \quad D = C = -ikV_{y0}, \\
B =& ikV_{y0} + \frac{2T_i ik^3 V_{y0}}{m_i \Omega_i^2}, \quad A = i + \frac{2T_i ik^2}{m_i \Omega_i^2}.
\end{aligned}
$$

In order to check the correctness of the calculations, we discuss the limiting cases by removing the dust particles from the system, i.e., by neglecting the dust density n_{d0}, dust temperature T_d and dust charge Z_d from the mathematical expressions. Under this situation, the term $2T_d k_d^2 n_{d0}$ from the coefficient F, the term $(2Z_d k_d n_{d0})/\varepsilon_0$ from the coefficients Λ, Q and M, the term $(2T_d kd)/(m_d \varepsilon_0)\partial_x n_{d0}$ from the coefficient P disappear and these coefficients take the form

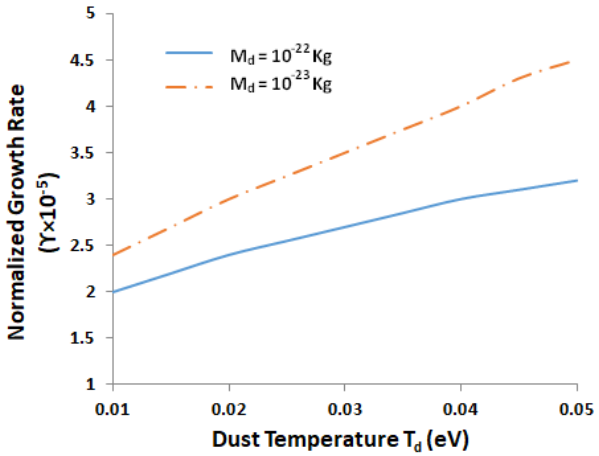

Figure 2. Variation of normalized growth rate of instability as a function of dust temperature for different mass of the dust, when $d = 5$ m, $\lambda = 5$ cm, $x = \lambda/4$, $n_{e00} = n_{i00} = 10^{18}$ m^{-3}, $n_{d0} = 5 \times 10^{11}$ m^{-3}, $T_i = 0.3$ eV, $T_e = 2.0$ eV, $m_i = 1.6 \times 10^{-27}$ kg, $V_{y00} = 10^3$ m/s, $U_{y00} = 10^5$ m/s, $B_0 = 1$ T and $Z_d = 1000$.

as obtained in Ref. [29] for the plasma system which is dust free. Quantitatively the coefficient F increases whereas the coefficients Λ, Q, M and P decrease in the absence of dust particles. These make a significant impact on the growth rate, which is clear when the present results are compared with the results of Ref. [29]. For example, the growth rate in the absence of the dust particle remains lower and hence, the dust particles also contribute positively and trigger the instability in the said systems. Since the results are reproduced when we neglect the dust density n_{d0}, dust temperature T_d and dust charge Z_d during the numerical calculations and the same results are obtained when these are removed from the mathematical expressions and a new dispersion equation is solved, this confirms that the present calculations are correct.

4. Results and discussion

Equation (11) is solved numerically for different parameters of the $\mathbf{E} \times \mathbf{B}$ plasma system. We make use of the Runge-Kutta method, the details of which are discussed in Refs. [14, 16, 31, 32]. The numerical solution gives several values of the angular frequency ω. The real vales of the frequency correspond to the propagation of the waves, whose velocity is found to be very less. However, we are interested in the complex values of the frequency as the negative and imaginary part of the complex frequency leads to the temporal growth of the wave. We calculate the normalized value of this frequency to study the variation of the growth rate of the instability. The normalization is done in terms of the ion plasma frequency. Figures 2-5 show the variation of this growth rate with different parameters of the dust and other plasma parameters.

Figure 2 shows that the growth rate increases with the dust temperature. This is because high temperature produces increased thermal motion and hence leads to the situation similar to the larger pressure gradient force. Since the cause

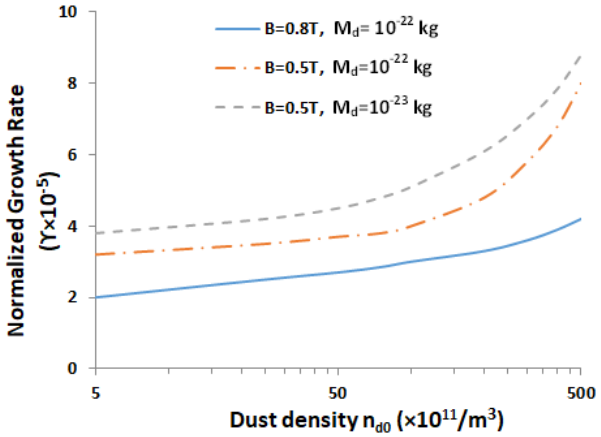

Figure 3. Variation of normalized growth rate of instability with the dust density for different values of magnetic field and dust mass, when $d = 5$ m, $\lambda = 5$ cm, $x = \lambda/4$, $n_{e00} = n_{i00} = 10^18$ m^{-3}, $T_i = 0.3$ eV, $T_e = 2.0$ eV, $T_d = 0.01$ eV, $m_i = 1.6 \times 10^{-27}$ kg, $V_{y00} = 10^3$ m/s, $U_{y00} = 10^5$ m/s and $Z_d = 1000$.

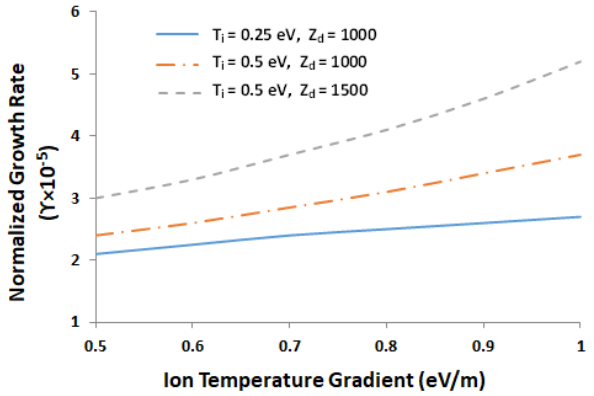

Figure 4. Normalized growth rate of the instability as a function of the ion temperature gradient (in eV/m) for different temperature of ions (T_i) in eV and different charge of dust, when $d = 5$ m, $\lambda = 5$ cm, $x = \lambda/4$, $n_{e00} = n_{i00} = 10^{18}$ m^{-3}, $M_d = 10^{-22}$ kg, $n_{d0} = 5 \times 10^{11}$ m^{-3}, $T_i = 0.3$ eV, $T_e = 2.0$ eV, $m_i = 1.6 \times 10^{-27}$ kg, $V_{y00} = 10^3$ m/s, $U_{y00} = 10^5$ m/s and $B_0 = 1$ T.

of this instability is the gradient, the enhanced dust temperature would in turn affect in the same manner as the stronger density gradients in the plasma, giving rise to the increased growth rate of the instability. This is also observed that the instability grows with higher rate when the dust particles have smaller mass. This is due to the enhanced restoring force. Moreover, the impact of the dust mass is much significant when the dust temperature is larger. These effects of dust temperature and dust mass are similar effects as obtained by Malik et al. [5] in a Hall thruster plasma when the dust exits in the exit region and only the electrons are magnetized. The impact of the size dust (generally in micrometers in the present systems) can also be understood based on the mass of the dust particles through Fig. 2, as the higher mass particles are expected to be larger in size. In this regard, instability grows with smaller rate in the presence of dust of higher mass and hence of the larger size.

Figure 3 depicts the effect of dust density, magnetic field and dust mass on the normalized growth rate. The growth rate increases at a slow pace when the dust density is increased. However, after a value greater than $2.5 \times 10^{11}/\text{m}^3$ the growth increases very significantly. This can also be seen that the stronger magnetic field reduces the growth rate, as has been observed by other investigators in a Hall thruster plasma [5, 10–12, 17, 18, 27, 28]. The dust mass also reduces the growth of the instability. It means the heavier dust grains suppress the instability in an $\mathbf{E} \times \mathbf{B}$ plasma system; similar to the case of Hall thruster where only the electrons are magnetized.

The charge of the dust can increase or fluctuate due to the finite electron and ion currents flowing in or out of the dust particles in the system. The currents develop due to the difference in the dust grain surface potential and the plasma potential. Other processes such as secondary emission, photoemission of electrons may also take place during the charging [33, 34]. Hence, in Figure 4, we uncover the role of ion temperature gradient on the growth rate of the instability for different values of the ion temperature and dust charge. At lower ion temperature, the instability grows a little slowly with the ion temperature gradient, but as the ion temperature increases the growth of the instability becomes significantly higher. This result is consistent with the observation made in a dust free plasma under the impact of cross-field [29, 30]. The additional observation is related to the effect of dust charge on the growth rate. Clearly the instability grows much faster in the plasma where the dust particles contain larger charge. This result matches with the observation of Malik et al. [5] in a Hall thruster plasma when the dust exits in the exit region. The physical reasoning behind this can be understood as follows. In the presence of higher dust charge, stronger Coulomb force exists in the system that leads to the faster growing instability inside the chamber.

This is seen that the growth rate of the instability is finite but lower for the lower values of the temperature gradient. While calculated the growth rate numerically after neglecting the temperature gradient a finite value of the growth rate is observed, confirming that the instability occurring in the present system is driven mainly by the density gradient. The above results show that the magnetic field suppresses the growth of the instability. Although we have considered a uniform magnetic field in the channel, it will be quite interesting to see the role of the gradient in this field. For example, if the work is extended considering the magnetic field profile similar to the field taken in other works [35–37]. Then one can focus on the impact of inhomogeneity of the field on the growth rate and also the perturbed potential associated with the unstable wave. In addition, the investigation can be further extended to the plasma having weakly relativistic species [38–40]. Not only this, but the dust charge also fluctuates in realistic situations and hence, the problem can be solved by taking into account the charge fluctuations in the calculations. The variable or fluctuating charge of the dust has been shown to enhance the nonlinearity of the

system, because of which the nonlinear solitary structures with higher amplitudes evolved in the plasma [33, 34].

5. Conclusion

The $\mathbf{E} \times \mathbf{B}$ plasma system having dust was investigated in this article for the occurrence of instability. A focus was on the variation of the normalized growth rate of the instability under the impact of temperature gradient present in the plasma at the scale length much lower than the dimension of chamber. It was found that the instability grows faster with the higher temperature gradient and higher temperatures of the ion and dust particles. The stronger magnetic field and the larger mass of the dust were found to suppress the instability. This work has application in plasma processing, specifically the inductively coupled plasma system, in this direction, we can optimize the system based on the results so that the instability does not grow and the plasma can be effectively used for the deposition or specified etching.

Conflict of interest statement:
The authors declare that they have no conflict of interest.

References

[1] T. Ohkawa. "Dust particles as a possible source of impurities in tokamaks". *Kakuyūgō kenkyū*, **37**:117, 1977.

[2] Ch. Hollenstein, W. Schwarzenbach, A. A. Howling, C. Courteillea nd J. L. Dorier, and L. Sansonnens. "Anionic clusters in dusty hydrocarbon and silane plasmas". *Journal of Vacuum Science and Technology A*, **14**:535, 1996.

[3] J. Winter, V. E. Fortov, and A. P. Nefedov. "Radioactive dust levitation and its consequences for fusion devices". *Journal of Nuclear Materials*, **509**:293, 2001.

[4] H. K. Malik, R. Srivastava, S. Kumar, and D. Singh. "Small amplitude dust acoustic solitary wave in magnetized two ion temperature plasma". *Journal of Taibah University for Science*, **14**:422, 2020.

[5] H. K. Malik, J. Tyagi, and D. Sharma. "Growth of Rayleigh instability in a Hall thruster channel having dust in exit region". *AIP Advances*, **9**:055220, 2013.

[6] A. Lazurenko, V. Viala, M. Prioul, and A. Bouchoule. "Experimental investigation of high-frequency drifting perturbations in Hall thrusters". *Physics of Plasmas*, **12**:13501, 2005.

[7] A. I. Smolyakov, W. Frias, Y. Raitses, and N. J. Fisch. "Gradient instabilities in Hall thruster plasmas". *Proc. 32nd Int. Electr. Propuls. Conf.*, **85**:016401, 2011.

[8] W. Frias, A. I. Smolyakov, I. D. Kaganovich, and Y. Raitses. "Long wavelength gradient drift instability in Hall plasma devices. I. Fluid theory". *Physics of Plasmas*, **19**:72112, 2012.

[9] E. Chesta, C. M. Lam, N. B. Meezan, D. P. Schmidt, and M. A. Cappelli. "A characterization of plasma fluctuations within a Hall discharge". *IEEE Transactions on Plasma Science*, **29**:582, 2001.

[10] J. B. Parker, Y. Raitses, and N. J. Fisch. "Transition in electron transport in a cylindrical Hall thruster". *Applied Physics Letters*, **97**:91501, 2010.

[11] A. A. Litvak, Y. Raitses, and N. J. Fisch. "Experimental studies of high-frequency azimuthal waves in Hall thrusters". *Physics of Plasmas*, **11**:1701, 2004.

[12] A. Kapulkin and M. M. Guelman. "Low-Frequency instability in near-anode region of Hall Thruster". *IEEE Transactions on Plasma Science*, **36**:2082, 2008.

[13] D. H. J. Godall. "High speed cine film studies of plasma behaviour and plasma surface interactions in tokamaks". *Journal of Nuclear Materials*, **111**:11, 1982.

[14] L. Malik and A. Tevatia. "Comparative analysis of aerodynamic characteristics of F16 and F22 combat aircraft using computational fluid dynamics". *Defence Science Journal*, **71**:137, 2021.

[15] A. K. Aria and H. K. Malik. "Studies on waves and instabilities in a plasma sheath formed on the outer surface of a space craft". *Physics of Plasmas*, **15**:043501, 2008.

[16] L. Malik, S. Rawat, M. Kumar, and A. Tevatia. "Simulation studies on aerodynamic features of Eurofighter Typhoon and Dassault Rafale combat aircraft". *Materials Today: Proceedings*, **38**:191, 2021.

[17] S. Singh and H. K. Malik. "Growth of low-frequency electrostatic and electromagnetic instabilities in a Hall thruster". *IEEE Transactions on Plasma Science*, **39**:1910, 2011.

[18] S. Singh, H. K. Malik, and Y. Nishida. "High frequency electromagnetic resistive instability in a Hall thruster under the effect of ionization". *Physics of Plasmas*, **20**:102109, 2013.

[19] H. K. Malik and S. Singh. "Resistive instability in a Hall plasma discharge under ionization effect". *Physics of Plasmas*, **20**:52115, 2013.

[20] E. Fernandez, M. K. Scharfe, C. A. Thomas, N. Gascon, and M. A. Cappelli. "Growth of resistive instabilities in $\mathbf{E} \times \mathbf{B}$ plasma discharge simulations ". *Physics of Plasmas*, **15**:12102, 2008.

[21] S. Sen, A. Fukuyama, and F. Honary. "Rayleigh Taylor instability in a dusty plasma". *Journal of Atmospheric and Solar-Terrestrial Physics*, **72**:938, 2010.

[22] L. Malik, M. Kumar, and I. V. Singh. "A three-coil setup for controlled divergence in magnetic nozzle". *IEEE Transactions on Plasma Science*, **49**:2227, 2021.

[23] L. Malik. "Tapered coils system for space propulsion with enhanced thrust: a concept of plasma detachment". *Propulsion and Power Research*, **11**:171, 2022.

[24] L. Malik. "Novel concept of tailorable magnetic field and electron pressure distribution in a magnetic nozzle for effective space propulsion". *Propulsion and Power Research*, **12**:59, 2023.

[25] L. Malik. "In-flight plume control and thrust tuning in magnetic nozzle using tapered-coils system under the effect of density gradient". *IEEE Transactions on Plasma Science*, **51**:1, 2023.

[26] H. K. Malik. *Laser-Matter Interaction for Radiation and Energy*. CRC Press, 2021.

[27] J. Tyagi, D. Sharma, and H. K. Malik. "Discussion on Rayleigh equation obtained for a Hall thruster plasma with dust". *Journal of Theoretical and Applied Physics*, **12**:227, 2018.

[28] J. Tyagi, S. Singh, and H. K. Malik. "Effect of dust on tilted electrostatic resistive instability in a Hall thruster". *Journal of Theoretical and Applied Physics*, **12**:39, 2018.

[29] Munish, R. Dhawan, R. Kumar, and H. K. Malik. "Density gradient driven instability in an $\mathbf{E} \times \mathbf{B}$ plasma system having temperature gradients". *Journal of Taibah University for Science*, **16**:725, 2022.

[30] Munish, R. Dhawan, D. Sharma, and H. K. Malik. "Influence of magnetic field and ionization on gradient driven instability in an $\mathbf{E} \times \mathbf{B}$ plasma". *Journal of Theoretical and Applied Physics*, **16**:162234, 2022.

[31] L. Malik, G. S. Saini, and A. Tevatia. *Handbook of Sustainable Materials: Modelling, Characterization, and Optimization. A Self-sustained Machine Learning Model to Predict the In-flight Mechanical Properties of a Rocket Nozzle by Inputting Material Properties and Environmental Conditions*. CRC Press, 2023.

[32] L. Malik, G. S. Saini, and A. Tevatia. *Handbook of Sustainable Materials: Modelling, Characterization, and Optimization. Sustainability of Wind Turbine Blade: Instantaneous Real-Time Prediction of Its Failure Using Machine Learning and Solution Based on Materials and Design*. CRC Press, 2023.

[33] R. Kumar, H. K. Malik, and K. Singh. "Effect of dust charging and trapped electrons on nonlinear solitary structures in an inhomogeneous magnetized plasma ". *Physics of Plasmas*, **19**:012114, 2012.

[34] H. K. Malik, R. Tomar, and R. P. Dahiya. "Conditions for reflection and transmission of an ion acoustic soliton in a dusty plasma with variable charge dust". *Physics of Plasmas*, **21**:072112, 2014.

[35] L. Malik, A. Escarguel, M. Kumar, A. Tevatia, and R. S. Sirohi. "Uncovering the remarkable contribution of lasers peak intensity region in holography". *Laser Physics Letters*, **18**:086003, 2021.

[36] L. Malik and A. Escarguel. "Role of the temporal profile of femtosecond lasers of two different colours in holography". *Europhysics Letters*, **124**:64002, 2019.

[37] L. Malik. "Dark hollow lasers may be better candidates for holography ". *Optics and Laser Technology*, **132**:106485, 2020.

[38] H. K. Malik and K. Singh. "Small amplitude soliton propagation in a weakly relativistic magnetized space plasma: electron inertia contribution". *IEEE Transactions on Plasma Science*, **33**:1995, 2005.

[39] K. Singh, V. Kumar, and H. K. Malik. "Electron inertia contribution to soliton evolution in an inhomogeneous weakly relativistic two-fluid plasma". *Physics of plasmas*, **12**:072302, 2005.

[40] H. K. Malik. "Ion acoustic solitons in a relativistic warm plasma with density gradient". *IEEE Transactions on Plasma Science*, **23**:813, 1995.